

Optical Study of  $\text{PbZrO}_3$  and  $\text{NaNbO}_3$  Single Crystals\*

F. JONA, G. SHIRANE, AND R. PEPINSKY

*X-Ray and Crystal Analysis Laboratory, Department of Physics, The Pennsylvania State University, State College, Pennsylvania*

(Received December 8, 1954)

The twinning of the antiferroelectric crystals  $\text{PbZrO}_3$  and  $\text{NaNbO}_3$  has been studied. Essential differences between this twinning and the domain structure of ferroelectric  $\text{BaTiO}_3$  have been observed. It is shown that both orthorhombic  $\text{PbZrO}_3$  and  $\text{NaNbO}_3$  are optically negative and the refractive index is smallest along the  $a$  axis, along which axis the main antiparallel ion shifts have been reported. The birefringence of the crystals has been measured as a function of the temperature up to the transition points, and compared with the temperature dependence of the spontaneous strain.

## I. INTRODUCTION

SOME crystals of the cubic perovskite type at higher temperatures are known to undergo, on cooling, phase transitions accompanied by dielectric anomalies. According to their behavior below the transition points, these crystals can be divided into two groups: ferroelectrics and antiferroelectrics.

Crystals of the first group are characterized by a pronounced anomaly of the dielectric constant at the transition temperature, below which they show a reversible spontaneous polarization. The most important crystal in this group is the well-studied  $\text{BaTiO}_3$ ,<sup>1</sup> which undergoes a phase transition at 120°C, being cubic above and polar-tetragonal below the transition temperature. Two subsequent phase changes are observed upon decreasing temperature: from polar-tetragonal to polar-orthorhombic at 5°C, and to polar-rhombohedral at -70°C. The crystal is thus spontaneously polarized first along a cubic edge, then along a face diagonal, and finally along a body diagonal. These polarizations are accompanied by strains which generally involve an extension in the direction of polarization and contractions perpendicular to it. Ferroelectric properties have also been found in  $\text{KNbO}_3$ ,<sup>2</sup>  $\text{PbTiO}_3$ ,<sup>3</sup> and  $\text{KTaO}_3$ .<sup>4</sup>

Crystals of the second group (antiferroelectrics) are characterized by phase changes in which the dielectric constants behave in a similar way as at a ferroelectric transition, but no hysteresis loops and no permanent polarization are found below the transition temperature. The transition is to a new nonpolar state, characterized by the existence of antiparallel dipole orientations within the lattice. The first crystal to be discovered in this group was  $\text{PbZrO}_3$ .<sup>5</sup> Similar properties were subsequently observed in  $\text{PbHfO}_3$ <sup>6</sup> and  $\text{NaNbO}_3$ .<sup>2,7</sup>

The properties of the antiferroelectric  $\text{PbZrO}_3$  have

been examined heretofore chiefly with polycrystalline ceramic samples. The dielectric constant of  $\text{PbZrO}_3$  shows a pronounced anomaly at 230°C, and yet no hysteresis loops can be observed below this temperature. The room temperature structure was first reported from powder photographs to be tetragonal<sup>8</sup> with lattice parameters  $a=4.159\text{Å}$  and  $c/a=0.988$ . The powder pattern contains some extra lines which can only be explained by assuming a multiple unit cell. A later x-ray and optical study<sup>9</sup> of some very minute crystals of  $\text{PbZrO}_3$ <sup>10</sup> revealed the true symmetry at room temperature to be orthorhombic, with the lattice parameters given in Table I. One of the original cubic axes becomes an orthorhombic  $c$  axis, and the other two orthorhombic axes lie at 45° to the cubic axes, as in the case of orthorhombic  $\text{BaTiO}_3$  (see Fig. 1). The x-ray study indicated antiparallel shifts of the Pb ions along the  $a$  axis, as shown in Fig. 2.

The orthorhombic  $b$  axis of  $\text{PbZrO}_3$  is exactly equal to  $2a$ ; i.e., there is no measurable shear distortion of the ideal cubic lattice in the  $ab$  plane. This peculiar point will be discussed later. If comparisons are to be made between  $\text{PbZrO}_3$  and  $\text{BaTiO}_3$ , the properties of  $\text{PbZrO}_3$  below 230°C should be compared with those of  $\text{BaTiO}_3$  between 0°C and -70°C.

The case of  $\text{NaNbO}_3$  is similar to that of  $\text{PbZrO}_3$ . The room temperature structure is also orthorhombic,

TABLE I. Lattice parameters of orthorhombic modification of perovskite-type crystals. Orthorhombic axes  $a$ ,  $b$ , and  $c$  are related to monoclinic parameters<sup>a</sup>  $a_0=b_0$ ,  $c_0$ , and  $\beta$  by:  $a=2a_0 \sin(\beta/2)$ ,  $b=2a_0 \cos(\beta/2) \times m$ ,  $c=c_0 \times n$ .

Crystal	$a$ (Å)	$b$ (Å)	$c$ (Å)	$a_0/c_0$	$\beta-90^\circ$
$\text{BaTiO}_3^b$	5.68	5.67	3.99	1.006	8'
$\text{KNbO}_3^c$	5.72	5.69	3.97	1.016	16'
$\text{PbZrO}_3^d$	5.88	$5.88 \times 2$	$4.10 \times 2$	1.012	$\sim 0$
$\text{NaNbO}_3^e$	5.57	5.51	$3.88 \times 4$	1.009	40'

<sup>a</sup>  $c_0$  designates monoclinic axis.

<sup>b</sup> See reference 12.

<sup>c</sup> See reference 13.

<sup>d</sup> See reference 9.

<sup>e</sup> H. D. Megaw, Proc. Phys. Soc. (London) **58**, 133 (1946).

<sup>9</sup> Sawaguchi, Maniwa, and Hoshino, Phys. Rev. **83**, 1078 (1951).

<sup>10</sup> The technique used for growing these crystals is not given in reference 9, but a private communication of these authors states that the crystals were grown from a binary melt of  $\text{PbZrO}_3$  and  $\text{PbCl}_2$ .

\* Research supported by contract with the Wright Air Development Center, and with the Signal Corps Engineering Laboratories.

<sup>1</sup> See, for example, A. von Hippel, Revs. Modern Phys. **22**, 221 (1950).

<sup>2</sup> B. T. Matthias and J. P. Remeika, Phys. Rev. **82**, 727 (1951).

<sup>3</sup> G. Shirane and S. Hoshino, J. Phys. Soc. Japan **6**, 265 (1951).

<sup>4</sup> Hulm, Matthias, and Long, Phys. Rev. **79**, 885 (1950).

<sup>5</sup> Sawaguchi, Shirane, and Takagi, J. Phys. Soc. Japan **6**, 333 (1951).

<sup>6</sup> G. Shirane and R. Pepinsky, Phys. Rev. **91**, 812 (1953).

<sup>7</sup> Shirane, Newnham, and Pepinsky, Phys. Rev. **96**, 581 (1954).

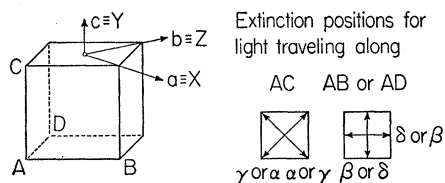


FIG. 1. Orthorhombic axes and axes of indicatrix in  $\text{PbZrO}_3$ .

and antiparallel ion shifts are observed within the  $ab$  plane.<sup>11</sup> The orthorhombic shear distortion is much larger than in  $\text{PbZrO}_3$ , however (see Table I).  $\text{NaNbO}_3$  has a cubic lattice of the perovskite type above 640°C. Upon cooling, it undergoes three phase changes: at 640°C, at 480°C, and at 360°C. The phases between these transition points both seem to be tetragonal. We will be concerned here mainly with the room-temperature orthorhombic modification.

Table I shows the lattice parameters of the orthorhombic phases of the ferroelectrics  $\text{BaTiO}_3$  and  $\text{KNbO}_3$ , and of the antiferroelectrics  $\text{PbZrO}_3$  and  $\text{NaNbO}_3$ .<sup>9,12,13</sup> For all of the crystals listed, the orthorhombic  $a$  axis is chosen to be along the direction of the main ion shifts. Parameters are also given in terms of a monoclinic lattice, for convenience in comparison of the distortions from the cubic lattice.

The present study was undertaken as a further step toward an understanding of the mechanisms of antiferroelectric transitions in perovskite type crystals. The preparation of single crystals of  $\text{PbZrO}_3$  is discussed, and the optical properties of these and of  $\text{NaNbO}_3$  single crystals are examined. Attention has been given to the type of twinning in these crystals.

## II. PREPARATION OF LEAD ZIRCONATE CRYSTALS

Severe evaporation of  $\text{PbO}$  at higher temperatures renders difficult the preparation of  $\text{PbZrO}_3$  crystals from the pure melt. To determine the extent of this evaporation, the following experiment was repeated at several temperatures. About 1 g of finely powdered  $\text{PbZrO}_3$  was placed in a covered Pt crucible; a globar oven was preheated to the specified temperature, after which the crucible was introduced, kept in it for one hour, and then removed. Cooling took place rapidly in air at room temperature. Results are presented in Table II.

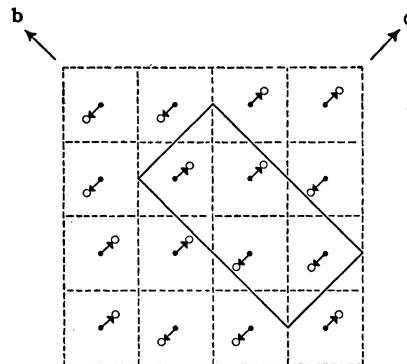
TABLE II. Loss of  $\text{PbO}$  by evaporation from  $\text{PbZrO}_3$  at high temperatures.

Firing temperatures in °C	% loss of $\text{PbO}$
1000	0.4
1100	3.5
1200	27.9
1300	53.7

<sup>11</sup> P. Vousden, *Acta Cryst.* 4, 545 (1951).

<sup>12</sup> H. F. Kay and P. Vousden, *Phil. Mag.* 40, 1019 (1949).

<sup>13</sup> P. Vousden, *Acta Cryst.* 4, 373 (1951).



Antiferroelectric structure of  $\text{PbZrO}_3$

FIG. 2. Antiferroelectric structure of  $\text{PbZrO}_3$ , according to Sawaguchi *et al.* (see reference 9). Arrows represent direction of shifts of  $\text{Pb}$  ions; solid line shows orthorhombic unit cell.

Because of this loss of  $\text{PbO}$ , resort was had to the method of binary melts, in order that the preparation temperature be as low as possible. Experiments were conducted to find the proper flux, the proper ratio of flux to  $\text{PbZrO}_3$ , and the most favorable temperature. The following fluxes were tried, the molar ratios of flux to  $\text{PbZrO}_3$  ranging from 10:1 to 1:1:— $\text{NaF}$ ,  $\text{NaCl}$ ,  $\text{KF}$ ,  $\text{KCl}$ ,  $\text{K}_2\text{CO}_3$ ,  $\text{RbCl}$ ,  $\text{B}_2\text{O}_3$ ,  $\text{AlF}_3$ ,  $\text{CaCl}_2$ ,  $\text{PbO}$ ,  $\text{PbCl}_2$ , and  $\text{PbF}_2$ . The maximum temperature was always lower than 1250°C. No crystals were obtained.

Small crystals of  $\text{PbZrO}_3$  have been obtained through the use of  $\text{PbF}_2$ , and recently also  $\text{PbCl}_2$ , as a flux, only for compositions close to the  $\text{PbZrO}_3$  side of the phase diagram. Best results were obtained with a molar ratio of  $\text{PbF}_2$  to  $\text{PbZrO}_3$  of 1:2 (e.g., 2.4 g  $\text{PbF}_2$ +6.9 g  $\text{PbZrO}_3$ ). The mixture was placed in a covered Pt crucible, introduced into the furnace at 1250°C, kept at this temperature for about one hour, and then cooled at the rate of 50°C/hour. The product appeared as a dense polycrystalline conglomerate, but isolated crystals were found attached to the walls of the crucible immediately above the surface of the conglomerate. Most of these crystals appear roughly cubic, about 0.3-mm edge length; occasionally octahedron shapes occur. They are transparent, of a light brown color, appear orthorhombic under the polarizing microscope, and show a transition to the cubic system at about 230°C.<sup>14,15</sup> The x-ray powder pattern is identical with that from a high-purity ceramic specimen of  $\text{PbZrO}_3$ .<sup>16</sup>

It appears that the crystals grow as a consequence of

<sup>14</sup> The dielectric behavior of high-purity ceramic specimens of  $\text{PbZrO}_3$  suggested the existence of an intermediate phase approximately between 225° and 233°C, on cooling only (see reference 15). Our optical investigation shows that this intermediate phase, if it exists, lies within less than one degree below the transition point; but our experimental arrangement is not able to confirm the existence of this phase within our crystals.

<sup>15</sup> Shirane, Sawaguchi, and Takagi, *Phys. Rev.* 84, 476 (1951).

<sup>16</sup> Our measurements give the following tetragonal parameters:  $a=4.161\pm 0.001\text{Å}$ ,  $c/a=0.988$ , in agreement with Megaw's results (see reference 8).

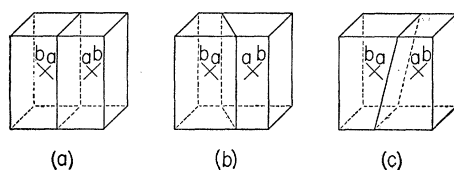


FIG. 3. Twinning of  $\text{PbZrO}_3$  crystals, showing symmetrical extinction: (a) Twinning on orthorhombic (110) plane. (b) Twinning on orthorhombic (111) plane. (c) Twinning on orthorhombic ( $hk0$ ) plane.

the evaporation of the solvent,  $\text{PbF}_2$ . The surface level of the melt decreases progressively and leaves crystals attached to the crucible walls. No  $\text{PbF}_2$  is detectable by x-ray patterns of the polycrystalline conglomerate; these show the  $\text{PbZrO}_3$  pattern only. The weight loss is about 22 percent of the starting total weight. Since the initial percentage of  $\text{PbF}_2$  by weight was about 62 percent, and if we assume that the loss in weight is almost entirely due to evaporation of  $\text{PbF}_2$ , we are left with about 4 percent of  $\text{PbF}_2$ , which is practically undetectable in the x-ray powder pattern.

Unfortunately, every attempt to control the evaporation of  $\text{PbF}_2$ , with the aim of growing larger crystals, was unsuccessful. Further research in this direction is in progress, as is the use of  $\text{PbCl}_2$  as a flux.

The extraction of the crystals from the crucible at the end of the growth process appears quite critical. The removal of  $\text{PbF}_2$  remaining in the end product by means of solution in strong acids is impossible because  $\text{PbZrO}_3$  itself undergoes a chemical reaction with these acids ( $\text{PbCl}_2$  is formed in  $\text{HCl}$ ,  $\text{PbSO}_4$  in  $\text{H}_2\text{SO}_4$ , etc.). A few crystals can be extracted by mechanical scratching. Platelike crystals are relatively easy to find. These are too small for dielectric measurements, but they are excellent for optical examination, twinning studies, and x-ray single-crystal examination.

The  $\text{NaNbO}_3$  crystals used for the optical measurements are the same crystals used for the previous dielectric and x-ray study.<sup>7</sup> They were grown using  $\text{NaF}$  as a flux.<sup>2</sup>

### III. TWINNING

$\text{PbZrO}_3$  crystals of about 0.3-mm edge length are always twinned, in a more or less complicated manner. The twin configuration can often be changed by heating the crystals to temperatures higher than the transition point,  $230^\circ\text{C}$ , and then cooling them rather rapidly. Slow cooling through the transition point sometimes reproduces the twin distribution existing before the heat treatment. The investigation of the influence of external stresses or fields on the twin boundaries could not be carried out because of the smallness of the crystals.

The twinning rules for nonpolar crystals arise from geometric conditions. In the case of polar crystals, electrostatic conditions may also be influential; the twin boundaries must be free of charge, and interaction

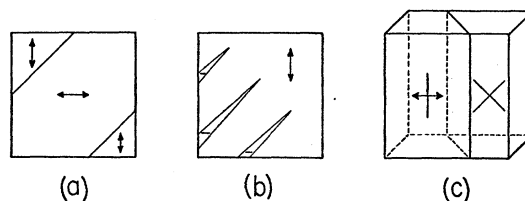


FIG. 4. Twinning on orthorhombic (111) plane in  $\text{PbZrO}_3$ : (a) Parallel extinction. (b) Parallel extinction: wedge laminae. (c) Mixed extinction: parallel and symmetrical. Double arrows show direction of orthorhombic  $c$  axis.

energy between the twins must be considered. In orthorhombic  $\text{BaTiO}_3$ , for example, the twinning of plates with symmetrical extinction takes place on an orthorhombic (110) plane<sup>12,17</sup> [see Fig. 3(a)]. Any plane (11 $l$ ) is possible, as far as the condition of no charge on the twin wall is considered, but the (110) plane would probably be preferred as a consequence of interaction energies; but geometrical considerations permit only (110). In  $\text{NaNbO}_3$ , which is certainly nonpolar,<sup>11</sup> geometrical conditions alone favor (110) as the twin plane of the orthorhombic lattice.

$\text{PbZrO}_3$  represents a particular case, since the length of the orthorhombic  $b$  axis is exactly twice that of the orthorhombic  $a$  axis. This renders (111) possible as a plane between twins with symmetrical extinction, on the basis of crystallographic considerations only. This twinning plane is observed in  $\text{PbZrO}_3$  crystals, but its existence is by itself not sufficient to exclude polarity. It is only the existence of twinning planes of the general type ( $hk0$ ) (with  $h, k \neq 1$ ), which can be considered as experimental evidence for the nonpolarity of the  $ab$  plane. The ( $hk0$ ) planes could not form domain walls, in the case of a ferroelectric crystal, even if they were allowable geometrically, because of the condition requiring no charge on the wall. This type of twinning plane has been observed in  $\text{PbZrO}_3$  sections with symmetrical extinction, proving the nonpolarity of the  $ab$  plane.

Orthorhombic  $\text{PbZrO}_3$  shows the following twinning, predominantly:

(1a) Plates with extinction parallel to the edges twin as represented schematically in Fig. 4(a); here double arrows indicate the direction of the orthorhombic  $c$  axis, which is in the plane of the drawing.

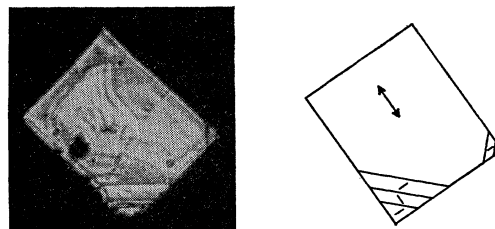
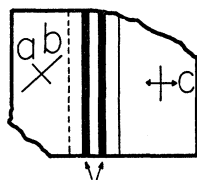
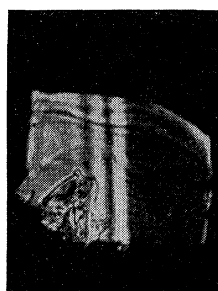
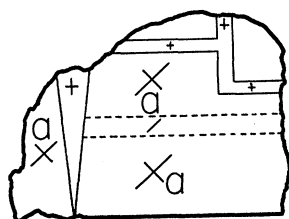
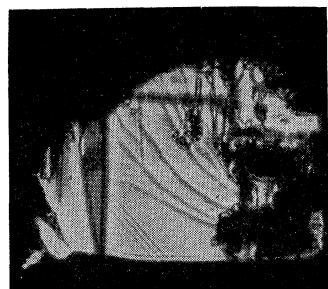


FIG. 5. Twinning of  $\text{PbZrO}_3$  crystals, showing parallel extinction.

<sup>17</sup> P. W. Forsbergh, Jr., Phys. Rev. **76**, 1187 (1949).



interference fringes

FIG. 6. Twinning of  $\text{PbZrO}_3$  crystals, showing parallel and symmetrical extinction.

The twin wall is parallel to a cubic (110) or orthorhombic (111) plane. Often, wedge twins as in Fig. 4(b) are visible. This is the type of twinning observed in orthorhombic  $\text{BaTiO}_3$ .<sup>12,17</sup> Figure 5 is a microphotograph of  $\text{PbZrO}_3$  showing this twinning.

(1b) Plates with mixed extinction positions (parallel and symmetrical) are twinned as represented in Fig. 4(c). This is the same as described in paragraph (1a), but as seen from a direction perpendicular to that of Fig. 4(a). Figure 6 shows this photographically in  $\text{PbZrO}_3$ .

(2) Plates with symmetrical extinction (at  $45^\circ$  to the cubic edges) are twinned as represented in Fig. 3(a), (b), (c). Figure 3(a) illustrates twinning in

$\text{PbZrO}_3$ , similar to that in  $\text{BaTiO}_3$  crystals as already discussed. In Fig. 3(b), the twin boundary is an orthorhombic (111) plane, which is only possible in  $\text{PbZrO}_3$  because of the peculiar relationship between the lengths of the orthorhombic axes ( $b=2a$ ). This twin configuration is assumed on the basis of the following experimental evidence. The twin components show extinction at  $45^\circ$  to the edges; the slow rays of the two twins are perpendicular to each other, as can be seen by inserting a unit retardation plate above the crystal lying between crossed nicols; the two twins are separated by a region which, in the position of maximum light intensity and in white light, shows decreasing interference color fringes towards the black central line of the region itself.

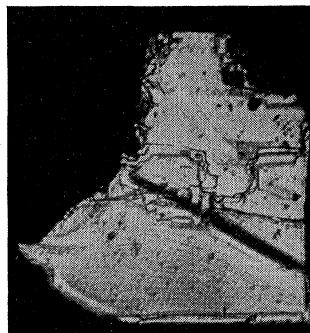
Finally, Fig. 3(c) shows twinning on an ( $hk0$ ) plane. This type of twinning was observed less often than types (a) and (b), and is again only possible in  $\text{PbZrO}_3$  because of the peculiar axial relationship and the nonpolarity in the  $ab$  plane. Photographs of  $\text{PbZrO}_3$  showing this twinning are given in Fig. 7.

#### IV. OPTICAL PROPERTIES

Orthorhombic untwinned crystals resulting from a small distortion of a cubic lattice can be divided into



(a)



(b)

FIG. 7. Twinning of  $\text{PbZrO}_3$  crystals with symmetrical extinction: (a) Interference fringes due to (111) walls are visible. (b) Other twin configuration of (a) after heating above the transition point.

two types, according to their extinction properties (see Fig. 1): (1) sections showing extinction parallel to the cube edges (parallel); (2) sections showing extinction at  $45^\circ$  to the cube edges (symmetrical).

Since these untwinned crystals are usually too small for study with conoscopic light, their properties can be analyzed as follows. Let  $n_a$ ,  $n_b$ ,  $n_c$  be the refractive indices of light waves vibrating along the crystallographic directions  $a$ ,  $b$ ,  $c$ . We wish to determine which of these indexes is the largest and which the smallest, i.e., which is  $\gamma$  and which is  $\alpha$ , where  $\alpha < \beta < \gamma$ ; this will establish the position of the axes of the indicatrix with respect to the crystallographic directions. The birefringence of the sections with symmetrical extinction is  $\Delta n_s = n_b - n_a$ ; that of the sections with parallel extinction is

$$\Delta n_p = n_c - \delta = n_c - \frac{n_a n_b \sqrt{2}}{(n_a^2 + n_b^2)^{\frac{1}{2}}}$$

Setting  $n_b = (1+x)n_a$ , where  $|x| \ll 1$ , and neglecting terms of second order,

$$\Delta n_p \cong n_c - \frac{1}{2}(n_a + n_b).$$

The sign of  $\Delta n_p$  can be determined experimentally in the following manner: for the sections showing mixed extinction [type 1(b) of the preceding section, Fig. 4(c) and the photograph in Fig. 6], the orthorhombic  $c$  axis must lie within the plane of the section and be perpendicular to the trace of the twin wall on the same plane. By using a quartz wedge, it can be proved that this direction is that of the slow ray, so that it follows that

$$n_c > \frac{1}{2}(n_a + n_b)$$

for both  $\text{PbZrO}_3$  and  $\text{NaNbO}_3$ .

The sign of  $\Delta n_s$  can be determined in the following way: consider a crystal showing two twins with symmetrical extinction, as in Fig. 3(a). In  $\text{NaNbO}_3$ , the angle distortion within the  $ab$  plane is  $40'$ . The direction of the  $a$  (or  $b$ ) axis can be identified by measuring the extinction positions of the two adjacent twins, which is  $40'$  from  $90^\circ$ . Then, by using a quartz wedge, it can be determined whether the identified direction is the fast or the slow ray. It appeared that the  $b$  direction is that of the slow ray, and thus it follows that

$$n_b > n_a.$$

In  $\text{PbZrO}_3$ , this method cannot be applied because  $2a = b$ ; thus there is no measurable angle distortion within the  $ab$  plane. We therefore picked out an untwinned crystal showing symmetrical extinction, and took an x-ray diffraction picture for rotation around the direction of the slow ray as identified with the quartz wedge. The measurement of the spacing showed that the rotation axis was the  $b$  axis, so that it follows again that

$$n_b > n_a.$$

The absolute magnitude of the birefringence  $\Delta n_s$  was examined by two methods. In Na light, interference fringes were produced in a wedge-shaped twin as shown in Fig. 4(c), the distance between the fringes was measured, the thickness of the crystal equivalent to a given path difference was calculated, and the birefringence was computed from the formula

$$R_{\mu\mu} = 10^3 \times (n_b - n_a) \times d_\mu,$$

where  $R_{\mu\mu}$  is the relative retardation in  $\mu\mu$ , and  $d_\mu$  is the thickness of the section in  $\mu$ . The second method was to measure the retardation  $R$  of a plane section by means of a calibrated quartz wedge (Na light), and the thickness  $d$  by means of the fine focussing adjustment on the microscope. The computation of  $(n_b - n_a)$  was then accomplished with the above formula.

Only this second method can be used for the measurement of  $\Delta n_p$  in  $\text{PbZrO}_3$ , because in this case the birefringence is too small to produce interference fringes in the thin plates; but both methods served for  $\text{NaNbO}_3$ .

The results of the measurements at room temperature are given in the first two columns of Table III, which also contains the corresponding values of orthorhombic  $\text{BaTiO}_3$ . In  $\text{BaTiO}_3$ , it was shown<sup>17</sup> by optical observations under application of an electric field that  $n_b > n_a$ . We could prove also, by means of the quartz wedge, that  $n_c > \frac{1}{2}(n_a + n_b)$ .<sup>18</sup>

We are now in the position to compute  $n_c - n_a \cong \Delta n_p + \frac{1}{2}\Delta n_s$  for the three crystals considered. The results are given in the third column of Table III. The relationship between  $n_a$ ,  $n_b$ ,  $n_c$  and  $\alpha$ ,  $\beta$ ,  $\gamma$  also appears clearly and is given in Table IV. It has to be seen that all three crystals are optically negative.

These conclusions were experimentally verified by the study of the largest possible untwinned crystals of  $\text{PbZrO}_3$  with conoscopic light. The sections with symmetrical extinction reveal an "optic normal" inter-

TABLE III. Some optical values for orthorhombic perovskite-type crystals.

	$\Delta n_p = n_c - \frac{n_a n_b \sqrt{2}}{(n_a^2 + n_b^2)^{\frac{1}{2}}}$	$\Delta n_s = n_b - n_a$	$\Delta n_p + \frac{1}{2}\Delta n_s \cong n_c - n_a$
$\text{PbZrO}_3$	0.005	0.039	0.024
$\text{NaNbO}_3$	0.084	0.080	0.124
$\text{BaTiO}_3^a$	0.046	0.075	0.083

<sup>a</sup> See reference 17.

TABLE IV. Orientation of indicatrices for orthorhombic perovskite-type crystals.

	$n_a$	$n_b$	$n_c$
$\text{PbZrO}_3$	$\alpha$	$\gamma$	$\beta$
$\text{NaNbO}_3$	$\alpha$	$\beta$	$\gamma$
$\text{BaTiO}_3$	$\alpha$	$\beta$	$\gamma$

<sup>18</sup> The optical study of Kay and Vousden (see reference 12) under application of an electric field seems to imply  $n_a > n_b > n_c$ , which is not in accordance with Forsbergh's and our own results.

ference figure, whereas the sections with parallel extinction appear to be almost normal to an optic axis. The optic axial angle does not differ much from  $90^\circ$ .

Some of the optical properties of  $\text{NaNbO}_3$  were studied by Wood.<sup>19</sup> The birefringence of the sections with symmetrical extinction was reported as 0.13, which is appreciably higher than our results. According to Wood, the orthorhombic  $c$  axis is the obtuse bisectrix. This last is in accord with our results, giving  $ac$  as the optic plane in  $\text{NaNbO}_3$ .

It is interesting to note that, for all of the crystals considered,  $n_a$  is the smallest refractive index. The  $a$  axis is the direction in which the main ion shifts were observed, parallel in  $\text{BaTiO}_3$ , and antiparallel in  $\text{PbZrO}_3$  and  $\text{NaNbO}_3$ . Furthermore, the crystals are optically negative, which characterizes once more the direction of the spontaneous polarization of the original cubic cell with respect to the directions perpendicular to it. It may be recalled that in tetragonal  $\text{BaTiO}_3$ ,  $n_c < n_a$ .

The value of the refractive index of  $\text{PbZrO}_3$  has been roughly estimated by using Chaulnes' method for determining the ratio between true and optical thickness; this gives the result  $\gamma \approx 2.2$ .

The temperature dependence of  $(\gamma - \alpha)$  and of  $[\beta - \alpha\gamma\sqrt{2}/(\alpha^2 + \gamma^2)^{1/2}] = (\beta - \delta)$  for  $\text{PbZrO}_3$  has been measured with the quartz wedge, with the results shown in Fig. 8.

Figure 9 shows the temperature dependence of the birefringences of  $\text{NaNbO}_3$  crystals, showing parallel and symmetrical extinctions. Above  $360^\circ\text{C}$ , all  $\text{NaNbO}_3$  crystals show parallel extinction, since the symmetry is tetragonal there.

## V. DISCUSSION

The temperature dependence of the birefringence of  $\text{PbZrO}_3$  and  $\text{NaNbO}_3$  is of interest because it is related to the spontaneous strains which take place below the transition points, and to the spontaneous polarizations

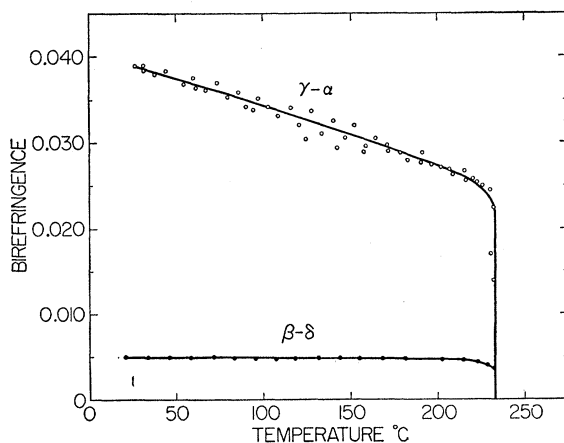


FIG. 8. Temperature dependence of birefringence of  $\text{PbZrO}_3$  crystals.

<sup>19</sup> E. A. Wood, *Acta Cryst.* **4**, 353 (1951).

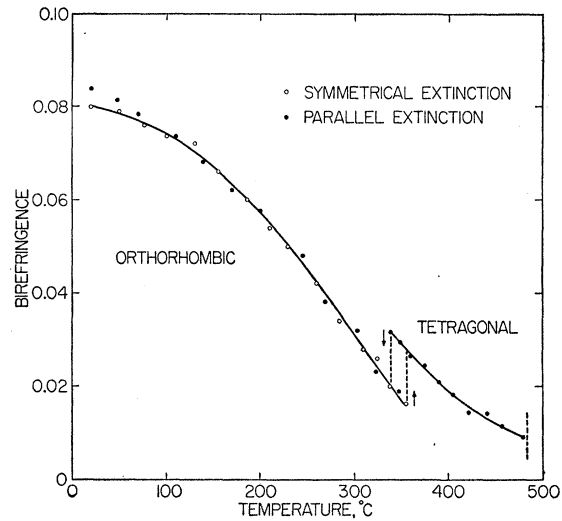


FIG. 9. Temperature dependence of birefringence of  $\text{NaNbO}_3$  crystals.

of the substructures. The treatment of the change in refractive index due to strain and polarization was first given by Pockels.<sup>20</sup> In the case of tetragonal  $\text{BaTiO}_3$ , this treatment was shown to give satisfactory results<sup>12,21</sup>; the birefringence of the tetragonal phase can be explained by the linear elasto-optic effect and by the spontaneous Kerr effect proportional to the square of the spontaneous polarization  $P_s$ . Since it was shown that the spontaneous strain is proportional to  $P_s^2$ ,<sup>22</sup> it was possible to establish a proportionality between the birefringence  $\Delta n$  and either the strain<sup>12</sup> or  $P_s^2$  alone.<sup>21</sup>

In principle, Pockels' treatment of the elasto-optic effect can be applied to a transition like that of  $\text{PbZrO}_3$  from cubic to orthorhombic. We assume that the following strains are introduced in the cubic  $\text{PbZrO}_3$ :

$$x_x = y_y, \quad z_z, \quad x_y.$$

We thus obtain for the birefringence of sections with symmetrical extinction

$$\gamma - \alpha \approx n^3 p_{44} x_y,$$

and for the birefringence of sections with parallel extinction

$$\beta - \delta \approx \frac{1}{2} n^3 (p_{11} - p_{12}) (x_x - z_z),$$

where  $n$  is the refractive index of the cubic phase, and the  $p_{ik}$  are the elasto-optical constants. The above results again neglect second order effects.

The formula for  $(\beta - \delta)$  appears to be reasonable, since it can be seen (Fig. 8) that  $(\beta - \delta)$  behaves quite similarly to  $(x_x - z_z)$ , i.e., in the first approximation, to  $(a_0/c_0 - 1)$ .<sup>23</sup> However, the behavior of  $(\gamma - \alpha)$ , which

<sup>20</sup> F. Pockels, *Lehrbuch der Kristallographie* (B. G. Teubner, Leipzig, 1906).

<sup>21</sup> W. J. Merz, *Phys. Rev.* **76**, 1221 (1949).

<sup>22</sup> A. F. Devonshire, *Phil. Mag.* **40**, 1040 (1949).

<sup>23</sup> E. Sawaguchi, *J. Phys. Soc. Japan* **7**, 110 (1952).

was found to be about eight times larger than  $(\beta - \delta)$  at room temperature, can hardly be explained by the above formula (assuming similar orders of magnitude and temperature behavior of all  $p_{ik}$ 's) because the shear  $x_y$  of orthorhombic  $\text{PbZrO}_3$  is extremely small, if it is present at all.

In the case of  $\text{NaNbO}_3$  the situation is similar: the value of the axial distortion  $(a_0/c_0 - 1)$ , as measured by x-rays,<sup>7</sup> diminishes about four times upon heating from room temperature to the transition point at 360°C. The birefringence of sections with parallel extinction shows the same behavior, and could therefore be explained in principle by the strains  $x_x$  and  $z_z$  only. The birefringence of sections with symmetrical extinction shows the same behavior, whereas the angle distortion as measured by x-rays<sup>7</sup> becomes only two times smaller, at the transition point, than at room temperatures—proving again that the elasto-optic effect alone cannot explain the experimental results.

The above treatment is evidently incomplete because the spontaneous strains in the crystal are essentially related to the antiparallel ion shifts, which in turn create antiparallel polarizations. Pockels' treatment of the elasto- and electro-optic effects is purely phenomenological and deals only with macroscopic stress, strain, field, and polarization. The treatment is valid for  $\text{BaTiO}_3$ , at least to the first approximation, because the spontaneous strain and polarization of the unit cell are equal to the macroscopic strain and polariza-

tion. In  $\text{PbZrO}_3$  and  $\text{NaNbO}_3$ , the situation is more complicated since the unit cell of the orthorhombic lattice contains 8 or 16 unit cells of the original cubic lattice, and the distortions of the latter are in general different from the macroscopic deformation. The crystal as a whole has no net polarization; a correct treatment should imply the separate consideration of the sublattices, which are polarized in antiparallel directions, and their superposition. However, no satisfactory comparison with the experimental data can be made unless we know the values of the elasto- and electro-optic constants involved.

The crystal structure of  $\text{PbZrO}_3$  as given by Sawaguchi *et al.*<sup>9</sup> presents the quite reasonable model of the antiparallel shifts of Pb ions along the  $a$  direction, and could also explain the large optical anisotropy in the  $ab$  plane. This structure, however, does not suggest why the lattice parameters are exactly  $2a = b$ . It might be that some other ions (such as oxygens) shift simultaneously in the  $b$  direction, so as to give a large optical and dielectric anisotropy within the  $ab$  plane while keeping  $b = 2a$ . In fact, both the space groups  $Pba2$  and  $Pbam$  proposed for  $\text{PbZrO}_3$  allow any shift of ions within the  $ab$  plane except for one each of  $O_x$  or  $O_y$ . A more detailed structural study is necessary, if light is to be shed on this matter.

The authors are greatly indebted to John McLaughlin for his assistance during the crystal preparation and the measurements.

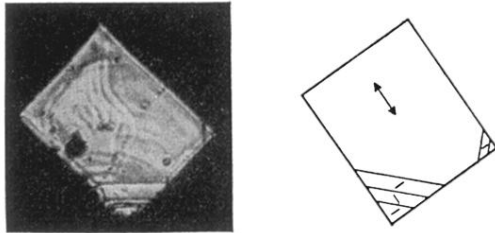
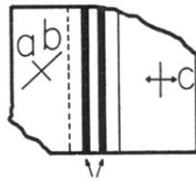
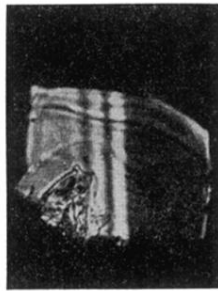
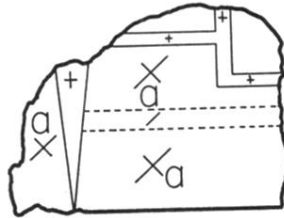
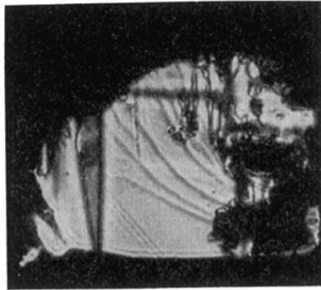


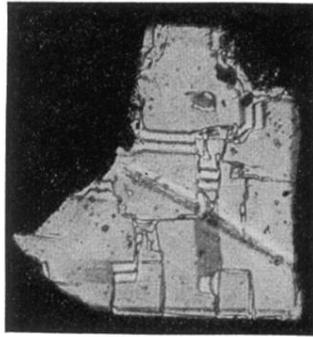
FIG. 5. Twinning of  $\text{PbZrO}_3$  crystals, showing parallel extinction.



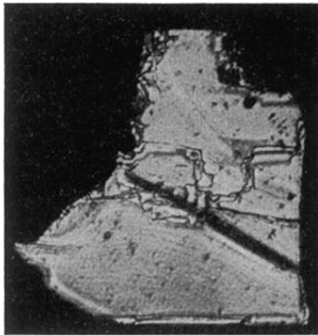


interference fringes

FIG. 6. Twinning of  $\text{PbZrO}_3$  crystals, showing parallel and symmetrical extinction.



(a)



(b)

FIG. 7. Twinning of  $\text{PbZrO}_3$  crystals with symmetrical extinction: (a) Interference fringes due to  $(111)$  walls are visible. (b) Other twin configuration of (a) after heating above the transition point.